On estimates for short wave stability and long wave instability in 3-layer Hele-Shaw flows

Prabir Daripa*

Department of Mathematics, Texas A&M University, College Station, TX-77843

April 19, 2011

Abstract

We consider linear stability of three-layer Hele-Shaw flows with each layer having constant viscosity and viscosity increasing in the direction of a basic uniform flow. While the upper bound results on the growth rate of long waves are well known from our earlier works, lower bound results on the growth rate of short stable waves are not known to-date. In this paper we obtain such a lower bound. In particular, we show in this paper following results: (i) the lower bound for stable short waves is also a lower bound for all stable waves and the exact dispersion curve for most stable eigenvalue intersects the dispersion curve based on the lower bound at a wavenumber where most stable eigenvalue is zero; (ii) the upper bound for unstable long waves is also an upper bound for all unstable waves and the exact dispersion curve for the most unstable eigenvalue intersects the dispersion curve based on upper bound at a wavenumber where the most unstable eigenvalue is zero. Numerical results are provided which support these findings.

Keywords: Hele-Shaw flows, Upper bound, Lower bound, Growth rates, Linear stability

*e-mail: prabir.daripa@math.tamu.edu

1 Introduction

The depth averaged velocity of a fluid flowing through the gap in a Hele-Shaw cell resembles the formula for the Darcy's law which is applicable to porous media flows. The viscous profile created due to rarefaction waves behind a sweeping front in two-phase immiscible flows in porous media can be modeled using a viscous profile behind the sweeping front in a Hele-Shaw flow. These analogies have motivated extensive studies in two-layer Hele-Shaw flows (see [1],[2], [3],[4]) to understand various issues related to porous media flows. Design of chemical enhanced oil recovery (EOR) processes usually involves flooding oil reservoirs with a sequence of displacing fluids of various compositions containing chemicals (see [5]). A close analogous system is multi-layer Hele-Shaw flows which has been recently studied by Daripa [6]. This same analogy motivates the current study of three-layer Hele-Shaw flows in order to gain an understanding of some of the complicated issues surrounding EOR technology.

The three-layer Hele-Shaw model consists of three different fluid phases in three distinct regions separated by sharp interfaces along which acts interfacial tensions. It is worth mentioning here that in actual porous media, the role of interfacial tension is more involved which results in diffuse two-phase regions, not a sharp interface across which act the interfacial tension (see [7]). Towards this end, we mention that linear stability of miscible displacement processes in porous media in the absence of dispersion has been studied earlier (see [8]). The approximation of diffused interfaces by sharp interfaces in our Hele-Shaw model allows exact studies of some hydrodynamic stability issues through analysis which play important roles in enhanced oil recovery. Many such issues related to three-layer Hele-Shaw flows have been studied by the author and his collaborators in recent years (see [6], [9], [10], [11]). In such flows of our present interest in this paper, there is a middle layer of fluid of constant viscosity μ between the displacing fluid of viscosity μ_l and the displaced fluid of viscosity μ_r. The viscosity μ is chosen so that $\mu_l < \mu < \mu_r$. Two initially planar interfaces including all three fluids in the three layers move with velocity U along the positive direction of x-axis. The y-axis is in the plane of the plates and extends all the way to infinity in both directions of the $y-$axis. In a frame moving with the velocity U, $x = 0$ and $x = -L$ are taken to be initial locations of the two planar interfaces with the displaced fluid extending all the way to $x = \infty$ and displacing fluid extending all the way to -∞. The interfacial tension at the leading interface at $x = 0$ is denoted by T and that at the trailing interface at $x = -L$ is denoted by S.

The eigenvalue problem arising from the linear stability analysis of this uniform flow

using equations relevant for Hele-Shaw flows has been derived in Daripa [11] and also in some references cited therein. This derivation is outlined here briefly. The disturbances $(\tilde{u}, \tilde{v}, \tilde{p})$ in basic velocity $(U, 0)$ and basic pressure P (see Daripa [11] for P) are first decomposed in normal modes according to the ansatz

$$(\tilde{u}, \tilde{v}, \tilde{p}) = (f(x), \phi(x), \psi(x))e^{(iky+\sigma\, t)} \tag{1}$$

where k is the wave number and σ is the growth rate. Then these are used in the linearized disturbance equations arising from Hele-Shaw flow equations and the linearized dynamic and kinematic boundary conditions. The resulting equations are then manipulated to obtain the following eigenvalue problem in $f(x)$. Details on this derivation can be found in Daripa [11].

$$f_{xx} - k^2 f = 0, \tag{2}$$

$$f_x^+(-L) = (\lambda\, r + s)f(-L), \quad f_x^-(0) = (\lambda\, p + q)f(0), \tag{3}$$

where $\lambda = 1/\sigma$ and r, s, p, q are given by

$$r = \{(\mu_l - \mu)Uk^2 + S\, k^4\}/\mu, \quad s = \mu_l k/\mu \geq 0, \tag{4}$$

$$p = \{(\mu_r - \mu)Uk^2 - T\, k^4\}/\mu, \quad q = -\mu_r k/\mu \leq 0. \tag{5}$$

Notice that the eigenvalue σ appears in the boundary conditions (3) through λ. There are two non-trivial eigenvalues $\sigma_+(k)$ and $\sigma_-(k)$ (where $\sigma_+(k) > \sigma_-(k)$) of this eigenvalue problem which has been discussed in Daripa [11].

Past works on this problem that are relevant for this paper are reviewed here briefly. This is also necessary for the purpose of continuity so that we place the contribution of this paper in proper perspective. An *absolute* upper bound on the growth rate has been derived in [9] and [10] in two different ways. In [9], this has been done using numerical analysis of the discrete version of the above eigenvalue problem followed by an application of Gerschgorin's localization theorem for eigenvalues. Since an absolute upper bound need not be the best upper bound (i.e., maximum growth rate), we sought to derive this by another approach hoping an improved upper bound can be obtained. In a subsequent paper [10], this was done using the variational formulation of the eigenvalue problem which is more elegant and straight-forward. Even though we have not emphasized in these two papers about the *local* upper bound on the growth rates of long waves, they are embedded in the content of those papers from which the *local* upper bound result for long waves follows. However, to-date no local lower bound result on the growth rates of short waves exists. This is partly due to the

fact that such short waves are stable due to surface tension effects. Therefore, it was felt at the time that the *local* lower bound for short waves may not be of interest. In retrospect, it turns out that this is not true for many reasons. Short waves participate and thus play an important role in determining overall stability in an experimental set up of finite (in y-direction) width of the plates. More importantly, we obtain in this paper stronger results: the local upper bound on the growth rates for most unstable modes which include the long waves and the local lower bound on the growth rates for most stable modes which include the short waves.

For our purposes below, we recall from [6] that σ is referred to as the growth rate even when $\sigma < 0$. Growth rate ($\sigma < 0$) characteristics of any short wave depend on the values of the parameters such as viscosity of three fluids, two interfacial tensions, and length of the middle layer. Therefore, growth rate of a short wave can vary widely in the space of these parameters. Even for a fixed set of parameter values, growth rate can decrease rapidly with increasing wave number. If a local lower bound on the growth rate for short waves also shares these same properties of the growth rate with respect to variation in one or more of these parameters, then it is possible to use the local lower bound to find approximately the qualitative effect of changes in parameter values on the stability of short waves. This quantitative information can be useful in the selection of one or more of the parameters appropriately in order to achieve some stabilization objectives of these short waves and in particular the system as a whole. In fact, its effect on the size of the unstable band (which usually is outside the band of short waves) can also be inferred in a qualitative sense, i.e., whether more or less number of unstable waves participate in determining stability of the system as the parameter values are changed. For example, if it is found from the *local* lower bound that the short waves as a group can become more stable from some changes in some parameter values, then it is very likely that the unstable band will also shrink in size.

Below, we first analyze the above eigenvalue problem to estimate this local lower bound for short waves. This can be done in three different ways all leading to the same result, and two of these three methods parallels the ones we have presented in [9] and [10] for estimating the *local* upper bound for long waves. Below we present all these three approaches to derive some inequalities from which not only the local lower bound on the growth rate for short waves but also the local upper bound on the growth rate of long waves follow. Some degree of overlap with the author's work in [9] and [10] is unavoidable but necessary in order to establish the equivalence among these three methods one of which is new. In this paper, we also compare these bounds with exact growth rates of these waves found numerically

in Daripa [6]. Such comparisons validate not only the bounds but also some other results derived below.

2 The estimates of the growth rate σ

Upper and lower bounds on the growth rates of short and long waves are derived in this section. We will later show that these are also the bounds on the growth rates for unstable and stable modes. This derivation will be based on the following proposition which we prove first. Recall $\lambda = 1/\sigma$.

Proposition 1. There are only following two possibilities.

$$a := \lambda p + q > 0, \qquad \text{or} \qquad b := \lambda r + s < 0. \tag{6}$$

Proof. The above result will be proved using three methods: (i) calculation using the general solution of (2); (ii) discretization of the stability system (2)-(3) and the Gerschgorin's localization theorem for eigenvalues; & (iii) variational formulation of the stability system.

(i) From calculation using the general solution of (2): The general solution of system (2)-(3) is given by

$$f(x) = A\, e^{kx} + B\, e^{-kx}, \tag{7}$$

where A and B satisfy the algebraic system

$$\left.\begin{aligned} &k(A - B) = (\lambda p + q)(A + B), \\ &k(A\, e^{-kL} - B\, e^{kL}) = (\lambda r + s)(A\, e^{-kL} + B\, e^{kL}). \end{aligned}\right\} \tag{8}$$

The above system has nontrivial solution A, B iff the determinant is zero, that is

$$(a - k)\, e^{kL}(b + k) - (a + k)\, e^{-kL}(b - k) = 0, \tag{9}$$

or

$$(ab - k^2)(e^{2kL} - 1) + k(a - b)(e^{2kL} + 1) = 0. \tag{10}$$

In [6], this algebraic equation has been solved for eigenvalues σ_+ and σ_- as a function of wavenumber k. Suppose that $a < 0$ and $b > 0$. Then both the terms in the left hand side of the above equation are negative and the sum can not equate to the right hand side which is zero. One can easily verify this and other possible scenarios from the Figure 1 and arrive at the conclusion (6). This figure shows zero level sets of $(ab - k^2)$ and $(a - b)$ using a and b as the two axis. The five curves in the figure then clearly identify regions when both $ab > k^2$ and $a > b$ hold or when both $ab < k^2$ and $a < b$ hold. These regions are shown shaded in

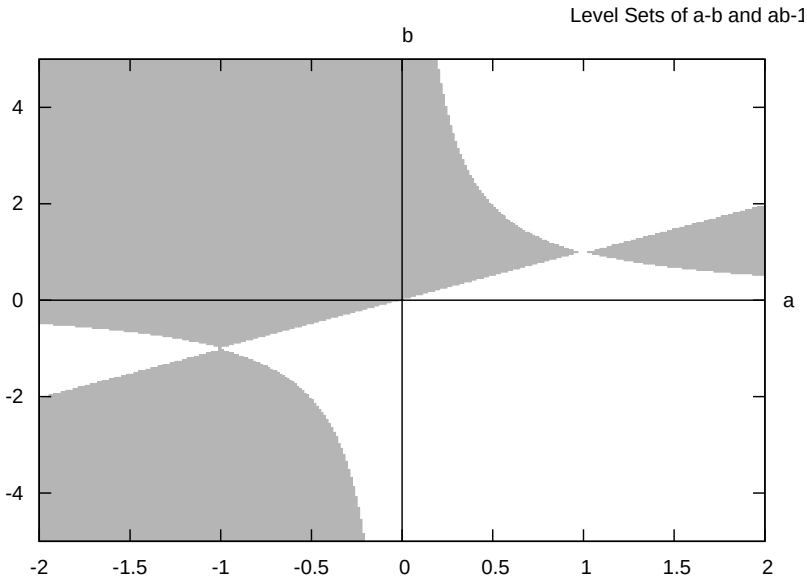

Figure 1: Plots of functions $a - b = 0$ and $ab - k^2 = 0$ for $k = 1$ with a and b as two axis. The regions where both $a - b > 0$ and $ab - k^2 > 0$ hold or both $a - b < 0$ and $ab - k^2 < 0$ hold are shaded.

the figure. These are then the regions in which the solution (a, b) of (10) can not lie, thus justifying the assertion (6).

(ii) From discretization of the stability system (2)-(3) and the Gerschgorin's localization theorem for eigenvalues: Discretization version of our paper is first recalled here from [9]. The domain $[-L, 0]$ is discretized into M subintervals of equal length $d = L/M$ by introducing the points $x_0 = 0, x_1 = -d, ..., x_i = -id, ..., x_M = -L$. The notation $f(x_i) = f_i$ is used. The derivative f_{xx} at the interior points $x_1, x_2, ..., x_{M-1}$ has been approximated as follows.

$$f_{xx}(x_i) \approx \frac{f(x_i + d) - 2f(x_i) + f(x_i - d)}{d^2}. \tag{11}$$

The end-point derivatives $f_x^-(x_0)$ and $f_x^+(x_M)$ are approximated as follows.

$$f_x(x_0) \approx \frac{f_0 - f_1}{d}, \quad f_x(x_M) \approx \frac{f_{M-1} - f_M}{d}, \tag{12}$$

Therefore the boundary conditions (3) become

$$(f_0 - f_1)/d = (\lambda p + q)f_0, \quad (f_{M-1} - f_M)/d = (\lambda r + s)f_M. \tag{13}$$

The discretized form of the stability system (2)- (3) is given by

$$E_{ij}f_j = F_{ij}f_j, \tag{14}$$

where E is the tridiagonal matrix with its entries given by

$$\begin{aligned} &E_{jj} = -2 \quad \text{except} \quad E_{0,0} = (1 - d\,q) \quad \text{and} \quad E_{M,M} = -(1 + ds), \\ &E_{j-1,j} = E_{j,j+1} = 1 \quad \text{except} \quad E_{0,1} = -1, \end{aligned} \tag{15}$$

and F is the diagonal matrix with its entries given by

$$F_{i,i} = d^2k^2 \quad \text{except} \quad F_{0,0} = \lambda d\,p \quad \text{and} \quad F_{M,M} = \lambda d\,r. \tag{16}$$

In the particular case $M = 4$, we have 3 equidistant interior points and the system (14) becomes

$$\left.\begin{aligned} &f_0(1 - d\,q) - f_1 = (\lambda d\,p)f_0, \\ &f_0 - 2f_1 + f_2 = d^2k^2 f_1, \\ &f_1 - 2f_2 + f_3 = d^2k^2 f_2, \\ &f_2 - 2f_3 + f_4 = d^2k^2 f_3, \\ &f_3 - f_4(1 + d\,s) = (\lambda d\,r)f_4. \end{aligned}\right\} \tag{17}$$

Using Gerschgorin's theorem, we obtain from (14)

$$|E_{kk} - F_{kk}| \leq \sum_{j \neq k} |E_{kj} f_j|/|f_k| \leq \sum_{j \neq k} |E_{kj}|,$$

if $\max |f_i| = |f_k|$. Now, following three possibilities exists.
(a) If $\max |f_i| = |f_j|,\ 0 < j < M$, then from (14) we obtain

$$|d^2k^2 + 2| \leq 2 \Rightarrow -4 \leq d^2k^2 \leq 0. \tag{18}$$

It is obvious that this last relation is false.

(b) If $\max |f_i| = |f_0|$, then we obtain

$$|\lambda d\,p - 1 + d\,q| \leq 1 \Rightarrow 0 \leq d(\lambda p + q) \leq 2. \tag{19}$$

(c) If $\max |f_i| = |f_M|$, then we obtain

$$|\lambda dr + 1 + d\,s| \leq 1 \Rightarrow -2 \leq d(\lambda r + s) \leq 0. \tag{20}$$

Thus we see that only the possibilities (b) and (c) are meaningful from which we again get the relation (6).

(iii) Multiplying equation (2) by $f(x)$ and then integrating the resulting equation in the interval $[-L, 0]$, we obtain after using the boundary conditions (3)

$$(\lambda p + q)f^2(0) - (\lambda r + s)f^2(-L) = \int_{-L}^{0} f_x^2\,dx + k^2 \int_{-L}^{0} f^2\,dx. \tag{21}$$

Therefore using the notations introduced in (6), we have

$$af^2(0) - bf^2(-L) \geq 0. \tag{22}$$

Suppose $a < 0$ and $b > 0$, then both terms in the above inequality are negative and the sum can not be positive. Therefore the assumption $a < 0$ and $b > 0$ is false and we obtain the result (6).

This completes the proof of the Proposition 1 in three different ways. □

We see from (5) that $p > 0$ if $0 < k < k_1$ and $p < 0$ if $k > k_1$ where $k_1^2 = U(\mu_r - \mu)/T$. Similarly from (4), $(-r) > 0$ if $0 < k < k_2$ and $(-r) < 0$ if $k > k_2$ where $k_2^2 = U(\mu - \mu_l)/S$. Therefore both $p > 0$ and $(-r) > 0$ hold when $0 < k < \min(k_1, k_2)$ (which we call "small" wavenumber below) and both $p < 0$ and $(-r) < 0$ hold when $k > \max(k_1, k_2)$ (which we call "large" wavenumber below). In the following we analyze these two cases: the case of "small" wavenumbers for which $p > 0$ and $(-r) > 0$ and the case of "large" wavenumbers for which $p < 0$ and $(-r) < 0$. We can see that (recall $\mu_l < \mu < \mu_r$)

$$p > 0 \quad \text{and} \quad (-r) > 0 \Leftrightarrow k^2 \leq \min\left\{\frac{U(\mu_r - \mu)}{T}, \frac{U(\mu - \mu_l)}{S}\right\}, \tag{23}$$

$$p < 0 \quad \text{and} \quad (-r) < 0 \Leftrightarrow k^2 \geq \max\left\{\frac{U(\mu_r - \mu)}{T}, \frac{U(\mu - \mu_l)}{S}\right\}. \tag{24}$$

We first consider the case of small wavenumbers. Then using (23) and *Proposition 1*, we obtain the following two possibilities.

$$\lambda > \frac{-q}{p} > 0 \Rightarrow \lambda > 0 \quad \text{and} \quad \sigma < \frac{p}{-q} = \frac{Uk(\mu_r - \mu) - k^3T}{\mu_r}, \tag{25}$$

or

$$\lambda > \frac{s}{-r} > 0 \Rightarrow \lambda > 0 \quad \text{and} \quad \sigma < \frac{-r}{s} = \frac{Uk(\mu - \mu_l) - k^3S}{\mu_l}. \tag{26}$$

Therefore, in this case we obtain the following upper bound σ_{ul} on the growth rate of long waves (i.e., small wavenumbers).

$$0 < \sigma < \sigma_{\text{ul}} = \max\left\{\frac{Uk(\mu_r - \mu) - k^3T}{\mu_r}, \quad \frac{Uk(\mu - \mu_l) - k^3S}{\mu_l}\right\}. \tag{27}$$

This upper bound for long waves is consistent with one of our results in [6]. There we have shown that σ_{ul} is an upper bound for all unstable waves (the word unstable was inadvertently left out from the third line after equation (33) in [6]), i.e. for all waves in the range

$$k \leq \max(k_1, k_2) = \max\left\{\sqrt{\frac{U(\mu_r - \mu)}{T}}, \sqrt{\frac{U(\mu - \mu_l)}{S}}\right\}. \tag{28}$$

This range contains all long waves and thus the upper bound result (27) for long waves is consistent with our result in [6]. It is easy to verify that $\sigma_{ul} = 0$ at $k = \max(k_1, k_2)$. We have also shown in Daripa [6] that $\sigma^+ = 0$ at $k = \max(k_1, k_2)$. Thus plots of σ_{ul} versus wavenumber k should intersect the dispersion curves $\sigma^+(k)$ at $k = \max(k_1, k_2)$ where $\sigma_{ul} = \sigma^+ = 0$. This along with the upper bound result (27) will be validated below numerically.

In the case of large wavenumbers for which (24) holds, the inequality signs in the relations (25) - (26) are reversed because $p, (-r)$ are negative. Therefore, the growth rate of short waves (i.e., large wave numbers) becomes negative and we obtain the following lower bound $\sigma_{\rm ls}$ for short waves.

$$0 > \sigma > \sigma_{\rm ls} = \min\left\{\frac{Uk(\mu_r - \mu) - k^3 T}{\mu_r}, \quad \frac{Uk(\mu - \mu_l) - k^3 S}{\mu_l}\right\}. \tag{29}$$

The new principal element of this paper is the last estimate (29) for short waves. It is also easy to verify that $\sigma_{ls} = 0$ at $k = \min(k_1, k_2)$. We have also shown in Daripa [6] that $\sigma^- = 0$ at $k = \min(k_1, k_2)$. This proves that the plot of σ_{ls} versus wavenumber k will intersect the dispersion curve $\sigma^-(k)$ at $k = \min(k_1, k_2)$ where $\sigma_{ls} = \sigma^- = 0$. This along with the lower bound result (29) are validated numerically in the next section.

3 Numerical Results

We have obtained above upper and lower bounds on the growth rates of short and long waves respectively but it turns out, as explained and justified above, these bounds also hold for all unstable and stable waves respectively. Since, in general, the bounds are rarely optimal allowing rooms for possible further improvement in these estimates through some different kind of analysis which we are not aware of at this point, it is useful to test the tightness of these bounds against exact calculations of the dispersion curves. In Daripa [6], such dispersion curves have been obtained numerically. The upper and lower bounds given above will now be compared with such numerically obtained exact dispersion curves.

In figures 2 through 5, we present plots for several choices of the set (S, T, U, L, μ) with viscosities of end layers fixed, namely $\mu_r = 10$ and $\mu_l = 2$. Figure 2(a) shows the plots of σ_+, σ_- & $\sigma_{\rm ul}$ versus k and Figure 2(b) shows the plots of σ_+, σ_- & $\sigma_{\rm ls}$ versus k for one such choice of the set: $(S, T, U, L, \mu) = (1, 1, 1, 1, 4)$. For the other three choices of the set (S, T, U, L, μ), such plots are shown in figures 3, 4, and 5 for $(S, T, U, L, \mu) = (1, 1, 1, 0.5, 4)$, $(S, T, U, L, \mu) = (1, 0.5, 1, 1, 4)$, and $(S, T, U, L, \mu) = (0.5, 1, 1, 1, 4)$ respectively. These figures support the validity of the estimates $\sigma_{\rm ul}$ and $\sigma_{\rm ls}$. Also, these figures support our results:

$\sigma_{ul} = \sigma^+ = 0$ at $k = \max(k_1, k_2)$ and $\sigma_{ls} = \sigma^- = 0$ at $k = \min(k_1, k_2)$. Validity of these have been confirmed for many many other choices of the set (S, T, U, L, μ).

The point of illustrating four typical cases is to have a qualitative idea of the trend of the difference between exact values of the growth rates and corresponding bounds as the parameters are varied. Giving more case studies than one usually tend to answer more questions that may otherwise arise in readers' mind. For example, from these typical case studies and associated figures 2-5, one finds that the plots of the upper bound $\sigma_{\rm ul}$ versus k in regions of interest (long wave regime) can have a double-hump or a single-hump characteristic (one being more pronounced than the other when there is a double hump). In figures 2(a), 3(a), 4(a), and 5(a), the upper bound plots shown by the dashed curves are not that far off from the exact growth rates σ_+ of most unstable waves which include very long waves. This leaves very little room for further improvement in the upper bound, specially when we consider the fact that the bound which does not depend on L has to hold for all values of L on which the growth rates depend, though the dependence of exact growth rates on L is exponentially small (see [6]). In Daripa [6], it has been shown that the quadratic equation whose solutions are σ_+ and σ_- contains a term involving e^{-kL} and none of the other terms in the equation depends on L. On the other hand, in figures 2(b), 3(b), 4(b), and 5(b), the lower bound shown by dashed curves agrees closely with the actual growth rates σ_- only for modest values of large wave numbers and quickly diverges away from the actual growth rates with increasing wavenumber. Thus, there is a lot of room for improving the lower bound result (29). It will be worthwhile in the future to take an attempt on improving upon this lower bound result.

In closing this section, it must be stressed that the bounds (27) and (29) are valid for any values of the parameters including $L > 0$. As discussed above, the large k regime for which the bound (29) holds corresponds to all stable modes which includes modest values of k as well as $k \to \infty$ (see Figures 2 through 5). In this asymptotic limit $k \to \infty$ with L finite, $kL \to \infty$ and in this limit, dispersion equation (9) gives either $a = k$ or $b = -k$. Using these values of a and b and the definitions of r, p, s, q from (4) and (5) in (6), it follows that

$$\sigma = [(\mu_r - \mu)Uk - Tk^3]/(\mu_r + \mu) < 0, \quad \text{or} \quad \sigma = [(\mu - \mu_l)Uk - Sk^3]/(\mu + \mu_l) < 0, \quad (30)$$

in the limit $k \to \infty$. This is consistent with the bound $\sigma_{\rm ls}$ given in (29) , keeping in mind that the value of this bound will be negative for large k. The two limiting values of σ given by (30) as $kL \to \infty$ are actually formulas for pure individual Saffman-Taylor growth rates of two individual interfaces. This makes sense because this limit also includes the limit $L \to \infty$ (for any finite k) when the instabilities of the two interfaces should be independent of each

other and should be driven by pure individual Saffman-Taylor instability, i.e., the eigenvalue corresponding to each of the two interfaces should be given by Saffman-Taylor formula with viscosity jump across that interface only.

4 Conclusions

We have derived here for the first time a lower bound $\sigma_{\rm ls}$ on the growth rate of short waves and re-derived an upper bound $\sigma_{\rm ul}$ on the growth rate of long waves. We have also shown that the lower bound is valid for all stable waves, i.e. $\sigma_{\rm ls} < \sigma^-$ for all $k > \min(k_1, k_2)$ and the upper bound is valid for all unstable waves, i.e. $\sigma_{\rm ul} > \sigma^+$ for all $k < \max(k_1, k_2)$. Therefore, we have provided here the upper bound on all most unstable modes (σ^+) and lower bound on all most stable modes (σ^-). Moreover, we have shown that $\sigma_{\rm ls} = \sigma^- = 0$ at $k = \min(k_1, k_2)$ and $\sigma_{\rm ul} = \sigma^+ = 0$ at $k = \max(k_1, k_2)$. These have been also validated using numerical results.

These results are useful in many ways. One can use these exact results without resorting to computation to qualitatively estimate the influence of changes of various parameters such as S, T, U and μ on the growth rates of stable and unstable waves. In [11], stabilization criteria has been given based on an absolute upper bound on the growth rate. However, this does not imply that a stabilized system based on an absolute upper bound (see [11]) will stabilize all individual modal disturbances. The lower and the upper bounds (27) and (29) for stable and unstable waves respectively can be used to determine the influence of such stabilization on any individual modal disturbance. There are many creative ways one can think of using these exact results. For example, following the exact procedure outlined in Daripa [11], one can find new stabilization criteria (i,e,, the values of S, T, μ) based on these local bounds rather than the absolute upper bound and purpose of doing so will be to target stabilization of specific stable or unstable wave.

We should mention in closing the limitations of the upper and lower bounds (27) and (29). These results are certainly valid for reasons mentioned before to predict the onset of instability. Moreover, these bounds contain all the parameters including both interfacial tensions which show that the interaction between the interfaces prevails even within the linearized theory. Thus, there is a transfer of instability between the interfaces regardless of how weak the interfacial disturbances are. As the disturbances grow and shapes of the interfaces change, nonlinearity comes into play and these bounds based on linear theory may not hold in the nonlinear regime. Nonetheless, it will be worthwhile to test this using

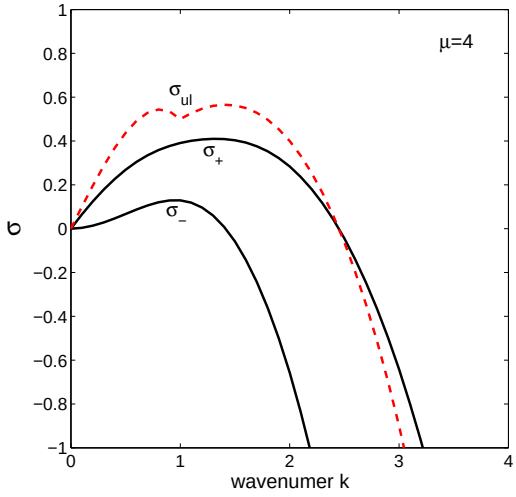

(a) Validation of the upper bound σ_{ul} for long waves.

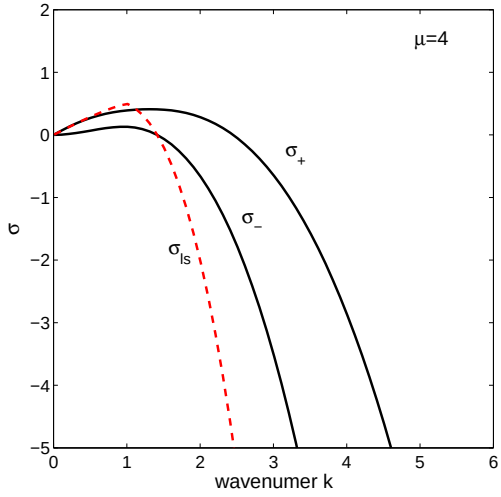

(b) Validation of the lower bound σ_{ls} for short waves.

Figure 2: Plots of $\sigma_+, \sigma_-, \&\sigma_{\text{ul}}$ versus k in the left subfigure (a). Similarly, plots of $\sigma_+, \sigma_-, \&\sigma_{\text{ls}}$ versus k in the right subfigure (b). The parameter values are $S = T = U = 1, L = 1$, and $\mu = 4$.

numerical as well as physical experiments which falls outside the scope of this paper.

5 Acknowledgments

We would like to thank the referees for making very helpful and constructive suggestions which have helped us to improve the paper. It is a pleasure to thank Gelu Pasa for his interest in this problem. We thank Xueru Ding for plotting the figures for us. This paper has been made possible by an NPRP grant from the Qatar National Research Fund (a member of The Qatar Foundation). The statements made herein are solely responsibility of the authors.

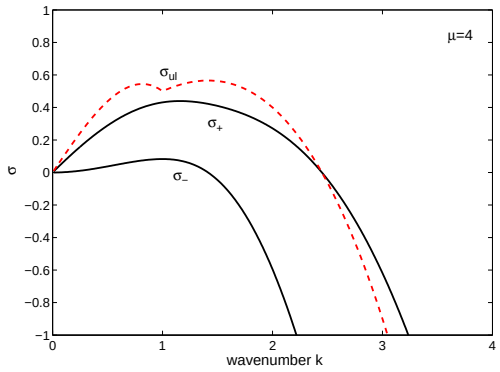

(a) Validation of the upper bound σ_{ul} for long waves.

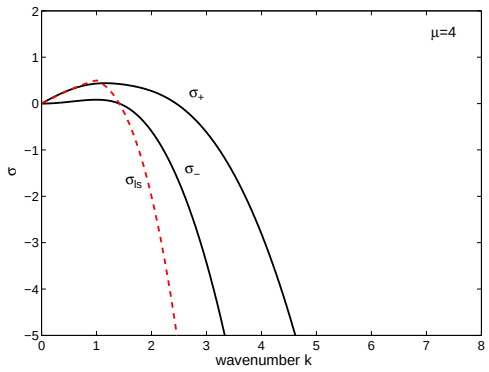

(b) Validation of the lower bound σ_{ls} for short waves.

Figure 3: Plots of $\sigma_+, \sigma_-, \& \sigma_{\text{ul}}$ versus k in the left subfigure (a). Similarly, plots of $\sigma_+, \sigma_-, \& \sigma_{\text{ls}}$ versus k in the right subfigure (b). The parameter values are $S = T = U = 1, L = 0.5$, and $\mu = 4$.

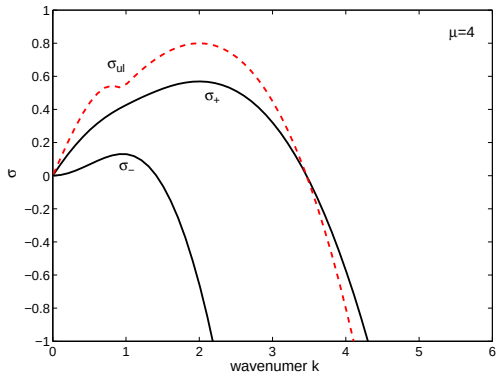

(a) Validation of upper bound σ_{ul} for long waves.

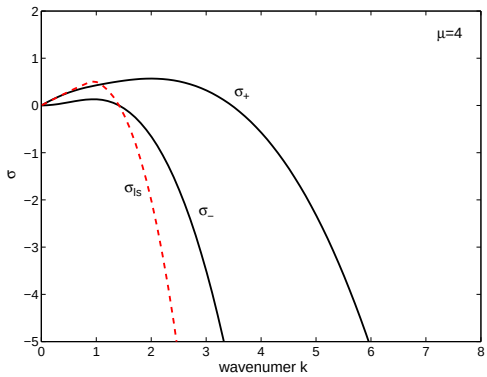

(b) Validation of the lower bound σ_{ls} for short waves.

Figure 4: Plots of $\sigma_+, \sigma_-, \& \sigma_{\text{ul}}$ versus k in the left subfigure (a). Similarly, plots of $\sigma_+, \sigma_-, \& \sigma_{\text{ls}}$ versus k in the right subfigure (b). The parameter values are $S = L = U = 1, T = 0.5$, and $\mu = 4$.

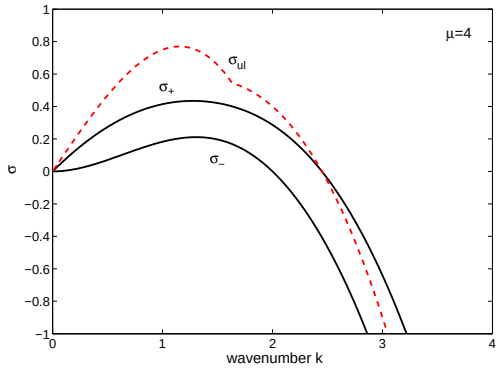

(a) Validation of upper bound $\sigma_{\rm ul}$ for long waves.

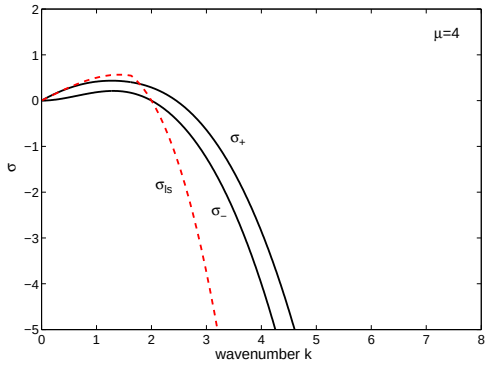

(b) Validation of the lower bound $\sigma_{\rm ls}$ for short waves.

Figure 5: Plots of $\sigma_+, \sigma_-, \& \sigma_{\rm ul}$ versus k in the left subfigure (a). Similarly, plots of $\sigma_+, \sigma_-, \& \sigma_{\rm ls}$ versus k in the right subfigure (b). The parameter values are $L = T = U = 1, S = 0.5$, and $\mu = 4$.

References

[1] P. G. Saffman, and G. I. Taylor, *The penetration of a fluid in a porous medium or Hele-Shaw cell containing a more viscous liquid*, Proc. Roy. Soc. London, A245, 312-329, (1958).

[2] P. G. Saffman, *Viscous fingering in Hele-Shaw cells*, J. Fluid Mech. **173** 73-94, (1986).

[3] G. M. Homsy, *Viscous fingering in porous media*, Ann. Rev. Fluid. Mech., **19**, 271-311, (1987).

[4] R. L. Chouke, P. van Meurs, and C. van der Poel, *The instability of slow, immiscible, viscous liquid-liquid displacements in permeable media*, Tran. AIME, 216:188, (1959).

[5] D. O. Shah, and R. S. Schechter (EDS.), Improved Oil Recovery By Surfactant and Polymer Flooding, Academic Press Inc., New York, (1977).

[6] P. Daripa, *Studies on stability in three-layer Hele-shaw flows*, Phys. of Fluids, 20, Article #112101, (2008).

[7] Y. C. Yortsos and F. J. Hickernell, *Linear stability of immiscible displacement in porous media*, SIAM J. Appl. Math., 49(3), (1989), pp. 730-748.

[8] F. J. Hickernell and Y. C. Yortsos, *Linear stability of miscible displacement processes in porous media in the absence of dispersion*, Stud. Appl. Math., 74, (1986), pp. 93-115.

[9] P. Daripa and G. Pasa, *On the Growth Rate for Three-Layer Hele-Shaw Flows: Variable and Constant Viscosity Cases*, Int. J. Engg. Sci., 43(11-12), pp. 877-884, 2005.

[10] P. Daripa and G. Pasa, *A simple derivation of an upper bound in the presence of viscosity gradient in three-layer Hele-Shaw flows*, J. Stat. Mech.: Theory and Experiment, No. P01014, January 2006.

[11] P. Daripa, *Hydrodynamic Stability of Multi-Layer Hele-Shaw Flows*, J. Stat. Mech., Article #P12005, (2008).